

Algorithm to estimate PAR from SeaWiFS data Version 1.2 - Documentation

Robert Frouin¹, Bryan Franz², and Menghua Wang²

¹*Scripps Institution of Oceanography, University of California San Diego, La Jolla*

²*SIMBIOS Project, NASA Goddard Space Flight Center, Greenbelt*

Algorithm description

The algorithm estimates daily (i.e., 24-hour averaged) Photosynthetically Active Radiation (PAR) reaching the ocean surface. PAR is defined as the quantum energy flux from the Sun in the spectral range 400-700 nm. It is expressed in Einstein/m²/day.

The PAR model uses plane-parallel theory and assumes that the effects of clouds and clear atmosphere can be de-coupled. The planetary atmosphere is therefore modeled as a clear sky atmosphere positioned above a cloud layer. This approach was shown to be valid by Dedieu et al. (1987) and Frouin and Chertock (1992). The great strength of such a de-coupled model resides in its simplicity. It is unnecessary to distinguish between clear and cloudy regions within a pixel, and this dismisses the need for often-arbitrary assumptions about cloudiness distribution.

Under solar incidence θ_s , the incoming solar flux at the top of the atmosphere, $E_0 \cos(\theta_s)$ is diminished by a factor $T_d T_g / (1 - S_a A)$ by the time it enters the cloud/surface system. In this expression, T_d is the clear sky diffuse transmittance, T_g is the gaseous transmittance, S_a is the spherical albedo, and A is the cloud/surface system albedo. As the flux, $E_0 \cos(\theta_s) T_d T_g / (1 - S_a A)$, passes through the cloud/surface system, it is further reduced by a factor A . The solar flux reaching the ocean surface is then given by

$$E = E_{clear} (1 - A) (1 - A_s)^{-1} (1 - S_a A)^{-1} \quad (1)$$

where A_s is the albedo of the ocean surface and $E_{clear} = E_0 \cos(\theta_s) T_d T_g$ is the solar flux that would reach the surface if the cloud/surface system were non reflecting and non-absorbing. In clear sky conditions, A reduces to A_s .

In order to compute E , A is expressed as a function of the radiance measured by SeaWiFS in the PAR spectral range (i.e., in bands 1 through 6). The algorithm works pixel by pixel and proceeds as follows.

First, for each pixel not contaminated by glitter the SeaWiFS radiance L_i^* in band i ($i = 1, 2, \dots, 6$), expressed in mW/cm²/μm/sr, is transformed into reflectance, R_i^* :

$$R_i^* = \pi L_i^* / [E_{0i} (d_0/d)^2 \cos(\theta_s^*)] \quad (2)$$

where E_{0i} is the extra-terrestrial solar irradiance in band i , θ_s^* is the sun zenith angle at the SeaWiFS observation time, and d_0/d is the ratio of mean and actual Earth-Sun distance. The glint areas are not selected because they would be interpreted as cloudy in the PAR algorithm.

Second, R_i^* is corrected for gaseous absorption, essentially due to ozone:

$$R_i' = R_i^*/T_{gi} \quad (3)$$

with

$$T_{gi} = \exp[-k_{oi}U_o/\cos(\theta_s^*)] \quad (4)$$

where k_{oi} is the ozone absorption coefficient in band i and U_o the ozone amount.

Third, the reflectance of the cloud/surface layer, R_i , is obtained from R_i' following Tanré et al. (1979) and assuming isotropy of the cloud/surface layer system. That is:

$$R_i = (R_i' - R_{ai})[T_{di}(\theta_s^*)T_{di}(\theta_v) + S_{ai}(R_i' - R_{ai})]^{-1} \quad (5)$$

where θ_v is the viewing zenith angle and R_{ai} is the intrinsic atmospheric reflectance in band i (corresponds to photons that have not interacted with the cloud/surface layer). The assumption of isotropy is made because no information on pixel composition is available.

In Eq. (5), R_a is modeled using the quasi single-scattering approximation:

$$R_a = (\tau_{mol}P_{mol} + \omega_{aer}\tau_{aer}P_{aer})[4\cos(\theta_s^*)\cos(\theta_v)]^{-1} \quad (6)$$

where τ_{mol} and τ_{aer} are the optical thicknesses of molecules and aerosols, P_{mol} and P_{aer} are their respective phase functions, and ω_{aer} is the single scattering albedo of aerosols. Subscript i has been dropped for clarity. The quasi single-scattering approximation is inaccurate at large zenith angles, but acceptable for the SeaWiFS sun zenith angles (less than 75 degrees). The diffuse transmittance T_d and spherical albedo S_a are computed using analytical formulas developed by Tanré et al. (1979):

$$T_d(\theta) = \exp[-(\tau_{mol} + \tau_{aer})/\cos(\theta)]\exp[(0.52\tau_{mol} + 0.83\tau_{aer})/\cos(\theta)] \quad (7)$$

$$S_a = (0.92\tau_{mol} + 0.33\tau_{aer})\exp[-(\tau_{mol} + \tau_{aer})] \quad (8)$$

where τ_{mol} is the optical thickness of molecules, τ_{aer} that of aerosols, and θ is either θ_s^* or θ_v .

The optical thickness of aerosols in band i , τ_{aeri} , is obtained from the optical thickness in band 8, τ_{aer8} , and the Angström coefficient between bands 4 and 8, α :

$$\tau_{aeri} = \tau_{aer8}(\lambda_8/\lambda_i)^\alpha \quad (9)$$

where λ_i and λ_8 are equivalent wavelengths in SeaWiFS bands i and 8, respectively. A monthly climatology based on three years of SeaWiFS data (1997-2000) is used for τ_{aer8} and α , since aerosol properties cannot be determined when the pixel is cloudy. This procedure is also justified because, in general, aerosol effects on E are secondary compared to cloud or θ_s effects.

To estimate ω_{aer} and P_{aer} , the two closest SeaWiFS aerosol models, k and l , that verify $\alpha(l) < \alpha < \alpha(k)$ are selected, and a distance $d_{aer} = [\alpha(l) - \alpha]/[\alpha(l) - \alpha(k)]$ is computed. Using this distance, ω_{aer} and P_{aer} are obtained as follows:

$$\omega_{aer} = d_{aer}\omega_{aer}(k) + (1 - d_{aer})\omega_{aer}(l) \quad (10)$$

$$P_{aer} = d_{aer}P_{aer}(k) + (1 - d_{aer})P_{aer}(l) \quad (11)$$

where $\omega_{aer}(l)$ and $\omega_{aer}(k)$ are the single scattering albedos of aerosol models l and k , and $P_{aer}(l)$ and $P_{aer}(k)$ their respective phase functions.

Next, an estimate of daily PAR, $\langle E \rangle_{day}$, is obtained by integrating Eq. (1) over the length of the day:

$$\langle E \rangle_{day} = \langle E_0 \rangle \int \left\{ \frac{\cos(\theta_s) \langle T_g \rangle \langle T_d \rangle [1 - \langle A \rangle]}{[1 - \langle A_s \rangle]^2 [1 - \langle S_a \rangle \langle A \rangle]} \right\} dt \quad (12)$$

with

$$\langle T_g \rangle = \langle T_{go} \rangle + \langle T_{gw} \rangle \quad (13)$$

$$\langle T_d \rangle = \sum_i (T_{di} E_{0i}) / \sum_i E_{0i} \quad (14)$$

$$\langle S_a \rangle = \sum_i (S_{ai} E_{0i}) / \sum_i E_{0i} \quad (15)$$

$$\langle A_s \rangle = \langle T_{dir} \rangle \langle T_d \rangle^{-1} [0.05 / (1.1 [\cos(\theta_s)]^{1.4} + 0.15)] + 0.08 \langle T_{dif} \rangle \langle T_d \rangle^{-1} \quad (16)$$

$$\langle T_{dir} \rangle = \sum_i T_{diri} E_{0i} / \sum_i E_{0i} \quad (17)$$

$$\langle T_{dif} \rangle = 1 - \langle T_d \rangle \quad (18)$$

$$T_{diri} = \exp[-(\tau_{moli} + \tau_{aeri}) / \cos(\theta_s)] \quad (19)$$

$$\langle A \rangle = F \langle R(t^*) \rangle \quad (20)$$

$$\langle R \rangle = \sum_i R_i(t^*) / \sum_i E_{0i} \quad (21)$$

where t^* is the SeaWiFS observation time, T_{diri} is the direct component of T_{di} in band i , and $\langle \rangle$ symbolizes average value over the PAR range.

In the expression of $\langle T_g \rangle$ (Eq. 13), the effect of both ozone and water ($\langle T_{go} \rangle$ and $\langle T_{gw} \rangle$, respectively) is modeled according to Frouin et al. (1989). Surface albedo is parameterized as a function of sun zenith angle and fractions of direct and diffuse incoming sunlight, following Briegleb and Ramanathan (1982). This parameterization, which takes into account Fresnel reflection and diffuse under-light, is sufficient since the influence of $\langle A_s \rangle$ on surface PAR is small. However, in some cases the retrieved $\langle A \rangle$ might be less than $\langle A_s \rangle$. When this happens, $\langle A \rangle$ is fixed to $\langle A_s \rangle$.

Even though the cloud/surface layer is assumed to be isotropic in the correction of clear atmosphere effects (Eq. 5), i.e., $A \approx R$, the dependence of A on sun zenith angle is

taken into account via the angular factor, F (Eq. 20). Instead of using for F angular models determined statistically (e.g., Young et al., 1998), analytical formulas proposed by Zege (1991) for non-absorbing, optically thick scattering layers are applied. The available angular models are fairly similar for partly cloudy, mostly cloudy, and overcast conditions, and they compare reasonably well with Zege's (1991) formulas.

The cloud/surface system, however, is assumed to be stable during the day and to correspond to the SeaWiFS observation. This assumption is crude, and PAR accuracy will be degraded in regions where clouds exhibit strong diurnal variability. Still, useful daily PAR estimates would be obtained by averaging in space and time. Note that the algorithm yields a daily PAR estimate for each instantaneous SeaWiFS pixel.

Finally, the individual daily PAR estimates, obtained in units of $\text{mW}/\text{cm}^2/\mu\text{m}$, are converted into units of $\text{Einstein}/\text{m}^2/\text{day}$ and averaged into 9 km resolution, daily, weekly, and monthly products. The factor required to convert units of $\text{mW}/\text{cm}^2/\mu\text{m}$ to units of $\text{Einstein}/\text{m}^2/\text{day}$ is equal to 1.193 to an inaccuracy of a few percent regardless of meteorological conditions (Kirk, 1994, pp. 4-8.). In middle and high latitudes, several daily estimates may be obtained over the same target during the same day, increasing product accuracy. Examples of PAR products are given in Fig. 1a (daily, December 10, 1997), Fig. 2a (weekly, December 3-10, 1997), and Fig. 3a (monthly, December 1997).

Algorithm evaluation

The SeaWiFS PAR estimates were compared with ISCCP PAR products for December 1997 (Fig. 1b, 2b, and 3b, respectively). The ISCCP products, provided by James Bishop, Columbia University, were generated using methods described by Bishop et al. (1997). Comparison statistics are displayed in Table 1. Agreement is good, with rms differences of 13.6(32.6%), 5.7(13.4%), and 3.6(8.4%) $\text{Einstein}/\text{m}^2/\text{day}$ on daily, weekly, and monthly time scales, and small biases on average (slightly higher ISCCP values). As expected, rms difference decreases with increasing time scale (uncertainties associated with cloudiness are reduced). The ISCCP values, however, tend to be systematically higher above 65 $\text{Einstein}/\text{m}^2/\text{day}$, and lower between 50 and 60 $\text{Einstein}/\text{m}^2/\text{day}$ (Fig. 4).

An evaluation of the SeaWiFS PAR estimates was performed using several years of in-situ PAR measurements from moored buoys off the west coast of Canada (Halibut Bank data set, 49.34N-123.73W) and in the central equatorial Pacific (ep1 data set, 0.00N-155.00W). James Gower, Institute of Ocean Sciences, Canada provided the Halibut bank data and Francisco Chavez, Monterey Bay Research Institute, the ep1 data. The total number of days used in the evaluation is 1387 (882 for ep1, 505 for Halibut bank). Scatter plots of SeaWiFS versus in-situ values are displayed in Figs. 5, 6, and 7 for daily, weekly, and monthly averages, respectively, and comparison statistics are summarized in Table 2. Agreement with in-situ measurements is good, with differences of 6.2(15.0%), 3.7(9.1%), and 3.3(8.1%) on daily, weekly, and monthly time scales when the ep1 and Halibut data sets are combined. The SeaWiFS estimates are higher by about 1 $\text{Einstein}/\text{m}^2/\text{day}$ at Halibut bank and by about 3 $\text{Einstein}/\text{m}^2/\text{day}$ at the ep1 location. Overestimation at the ep1 location is due to less cloudiness at local noon (about the time of satellite overpass) than during the afternoon. A further verification was made using 16 days of data collected at the BBOP site off Bermuda (courtesy of David Siegel,

University of Santa Barbara). Similar statistics were obtained for daily values, i.e., a rms difference of 5.6(16%) Einstein/m²/day and a negligible bias.

The results presented above indicate good algorithm performance. One should be aware of the limitations of the algorithm, which ignores the diurnal variability of clouds. This variability will be introduced statistically, as a function of geographic location and month of year, in a future, improved version of the algorithm.

Changes from version 1.1

In version 1.1 of the code, the retrieved albedo of the cloud/surface system, $\langle A \rangle$, could be lower than the surface albedo, $\langle A_s \rangle$, because of uncertainties in the modeling ($\langle A \rangle$ should always be greater or equal to $\langle A_s \rangle$; see Eq. 1). In version 1.2, $\langle A \rangle$ is forced to $\langle A_s \rangle$ when $\langle A \rangle$ is less than $\langle A_s \rangle$.

In version 1.1 of the code, absorption by water vapor was neglected in the computation of daily PAR (Eq. 12), because it occurs weakly in the PAR spectral range. In version 1.2, water vapor absorption is included according to Frouin et al. (1989). The vertically integrated water vapor amount is interpolated in time and space from the nearest available NCEP data.

Due to the above changes, daily PAR values obtained using version 1.2 may be smaller by a few percent, especially in clear sky conditions. Version 1.2 was implemented on 29 March 2001. Prior to that date, the available PAR products were generated using version 1.1. During the next SeaWiFS re-processing, the PAR products for the entire SeaWiFS period will be generated using version 1.2.

References

Bishop, J. K. P., W. B. Rossow, and E. G. Dutton, 1997: Surface solar irradiance from the International Satellite Cloud Climatology Project 1983-1991. *J. Geophys. Res.*, **102**, 6883-6910.

Briegleb, B. P., and V. Ramanathan, 1982: Spectral and diurnal variations in in clear sky planetary albedo. *J. Climate Appl. Meteor.*, **21**, 1168-1171.

Dedieu, G. P.-Y. Deschamps, and Y. H. Kerr, 1987: Satellite estimation of solar irradiance at the surface of the earth and of surface albedo using a physical model applied to Meteosat data. *J. Climate Appl. Meteor.*, **26**, 79-87.

Frouin, R., D. W. Lingner, K. Baker, C. Gautier, and R. Smith, 1989: A simple analytical formula to compute clear sky total and photosynthetically available solar irradiance at the ocean surface. *J. Geophys. Res.*, **94**, 9731-9742.

Frouin, R., and B. Chertock, 1992: A technique for global monitoring of net solar irradiance at the ocean surface. Part I: Model. *J. Appl. Meteor.*, **31**, 1056-1066.

Kirk, J. T. O., 1994: Light and photosynthesis in aquatic ecosystems, 2nd edition, Cambridge University Press, 509 pp..

Tanré, D., M. Herman, P.-Y. Deschamps, and A. De Leffe, 1979: Atmospheric modeling for space measurements of ground reflectances, including bi-directional properties. *Appl. Optics*, **18**, 3587-3594.

Young, D. F., P. Minnis, D. R. Doelling, G. G. Gibson, and T. Wong, 1998: Temporal interpolation methods for the clouds and Earth's Radiant Energy System (CERES) experiment. *J. Appl. Meteor.*, **37**, 572-590.

Zege, E. P., A. P. Ivanov, and I. L. Katsev, 1991: Image transfer through a scattering medium. Springer-Verlag, New York, 349 pp.

Table 1: SeaWiFS PAR versus ISCCP PAR

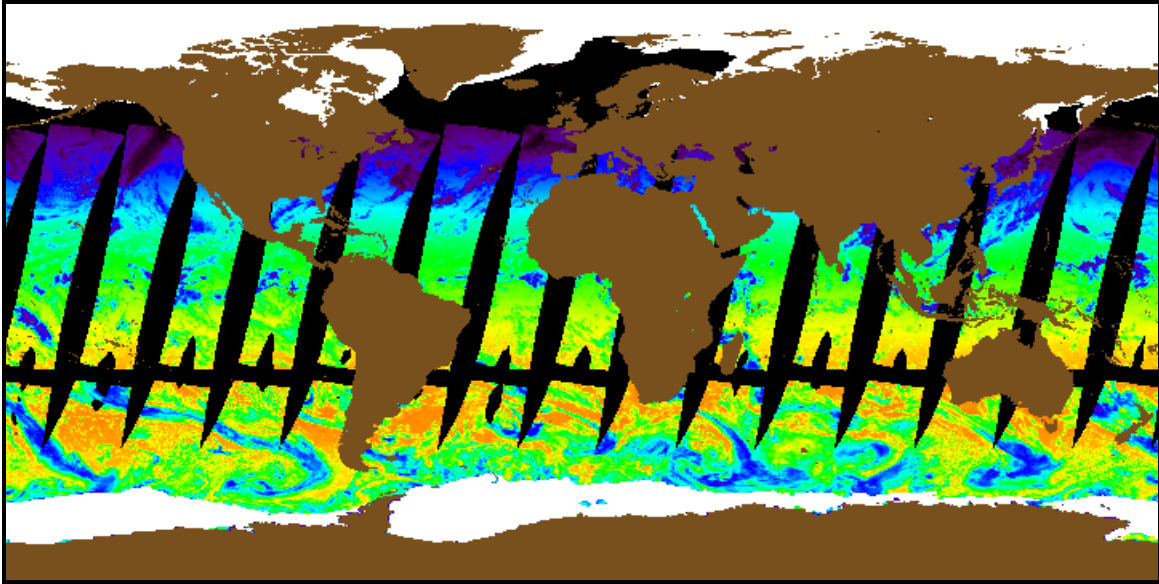
Averaging Period	Daily	8-Day	Monthly
correlation coefficient, r^2	0.587	0.881	0.954
bias, $E m^{-2} Day^{-1}$	-0.6 (-1.3%)	-0.8 (-1.9%)	-0.7 (-1.8%)
r.m.s. difference, $E m^{-2} Day^{-1}$	13.6 (32.6%)	5.70 (13.4%)	3.57 (8.4%)
mean, $E m^{-2} Day^{-1}$	41.6	42.7	42.3
number of points	89810	123015	123149

Table 2: SeaWiFS PAR versus *in situ* PAR

Averaging Period	Daily	8-Day	Monthly
Halibut Bank			
correlation coefficient, r^2	0.904	0.984	0.994
bias, $E m^{-2} Day^{-1}$	0.932 (3.3%)	0.863 (3.1%)	1.10 (4.1%)
r.m.s. difference, $E m^{-2} Day^{-1}$	6.2 (21.7%)	2.3 (8.2%)	1.8 (6.5%)
mean, $E m^{-2} Day^{-1}$	28.4	28.2	27.2
number of points	505	54	24
ep1			
correlation coefficient, r^2	0.613	0.680	0.673
bias, $E m^{-2} Day^{-1}$	2.9 (6.0%)	2.8 (5.8%)	2.8 (5.8%)
r.m.s. difference, $E m^{-2} Day^{-1}$	6.2 (12.8%)	4.3 (8.9%)	3.9 (8.0%)
mean, $E m^{-2} Day^{-1}$	48.7	48.3	49.0
number of points	882	103	38
Halibut Bank and ep1 Combined			
correlation coefficient, r^2	0.883	0.957	0.978
bias, $E m^{-2} Day^{-1}$	2.2 (5.3%)	2.1 (5.2%)	2.2 (5.4%)
r.m.s. difference, $E m^{-2} Day^{-1}$	6.2 (15.0%)	3.7 (9.1%)	3.3 (8.0%)
mean, $E m^{-2} Day^{-1}$	41.3	41.4	40.6
number of points	1387	157	38

Figure 1: SeaWiFS and ISCCP Global PAR Images, Daily Average.

a. SeaWiFS PAR, Daily Average, December 10, 1997



b. ISCCP PAR, Daily Average, December 10, 1997

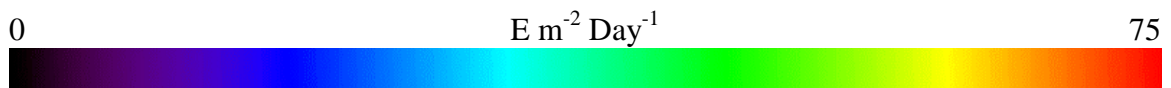
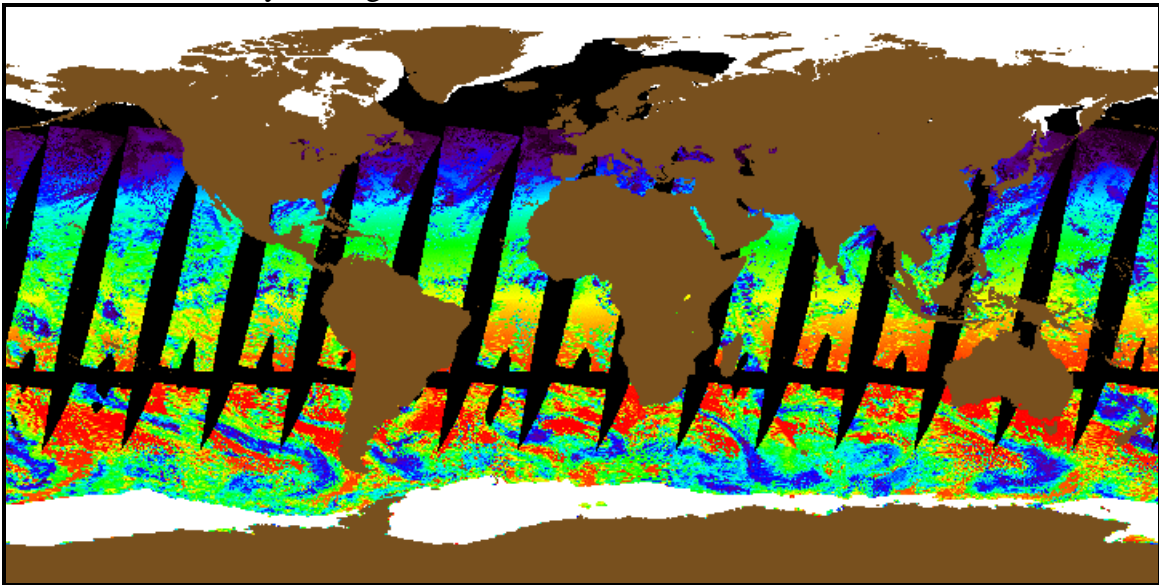
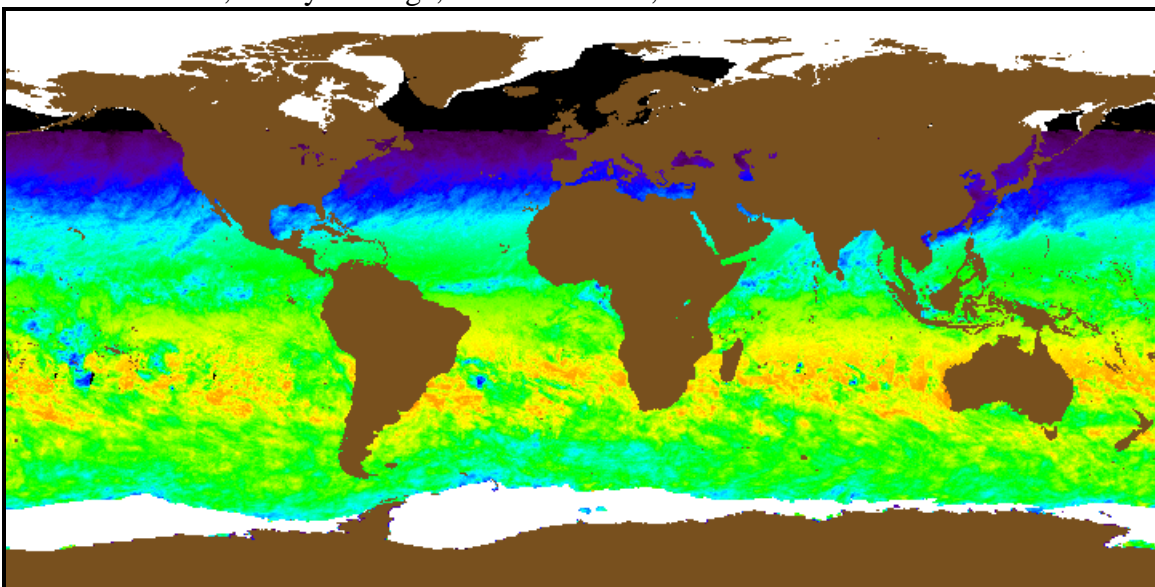


Figure 2: SeaWiFS and ISCCP Global PAR Images, 8-Day Average.

a. SeaWiFS PAR, 8-Day Average, December 3-10, 1997



b. ISCCP PAR, 8-Day Average, December 3-10, 1997

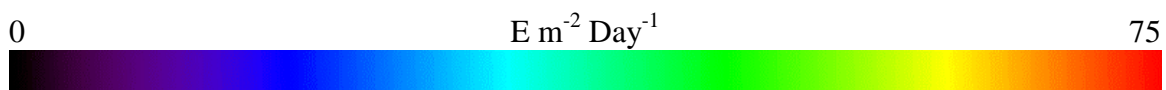
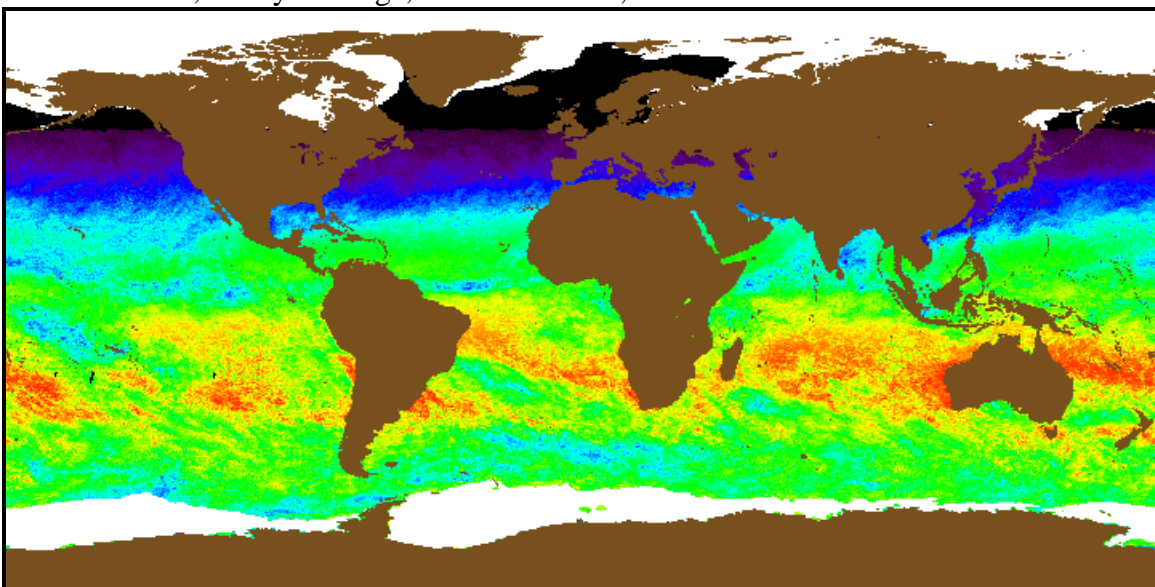
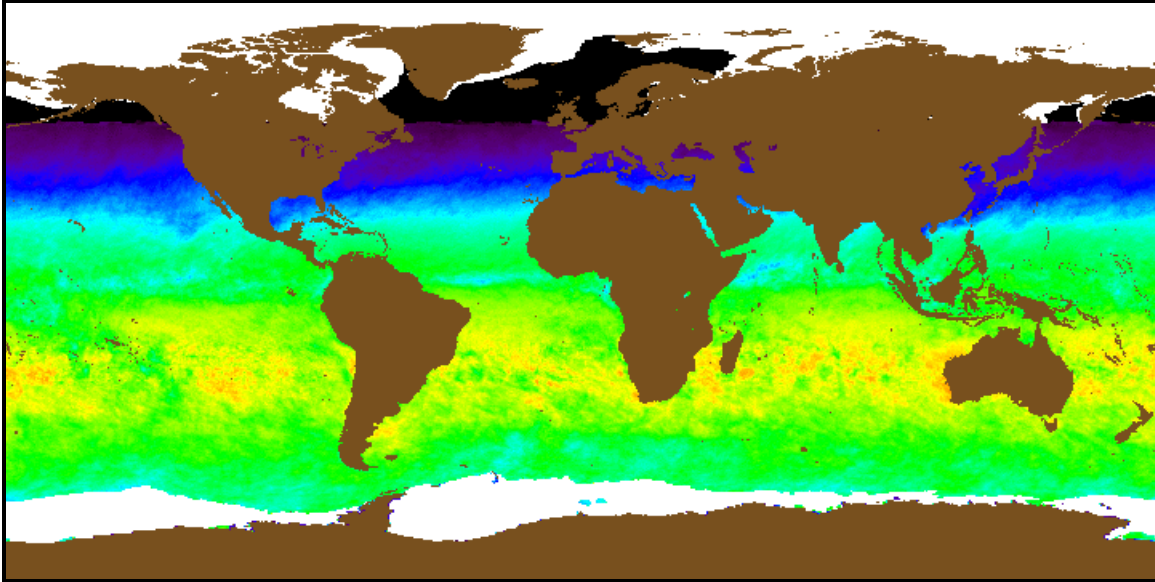


Figure 3: SeaWiFS and ISCCP Global PAR Images, Monthly Average.

a. SeaWiFS PAR, Monthly Average, December 1997



b. ISCCP PAR, Monthly Average, December 1997

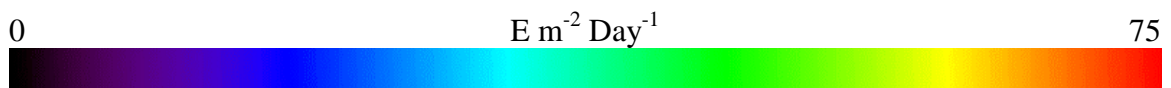
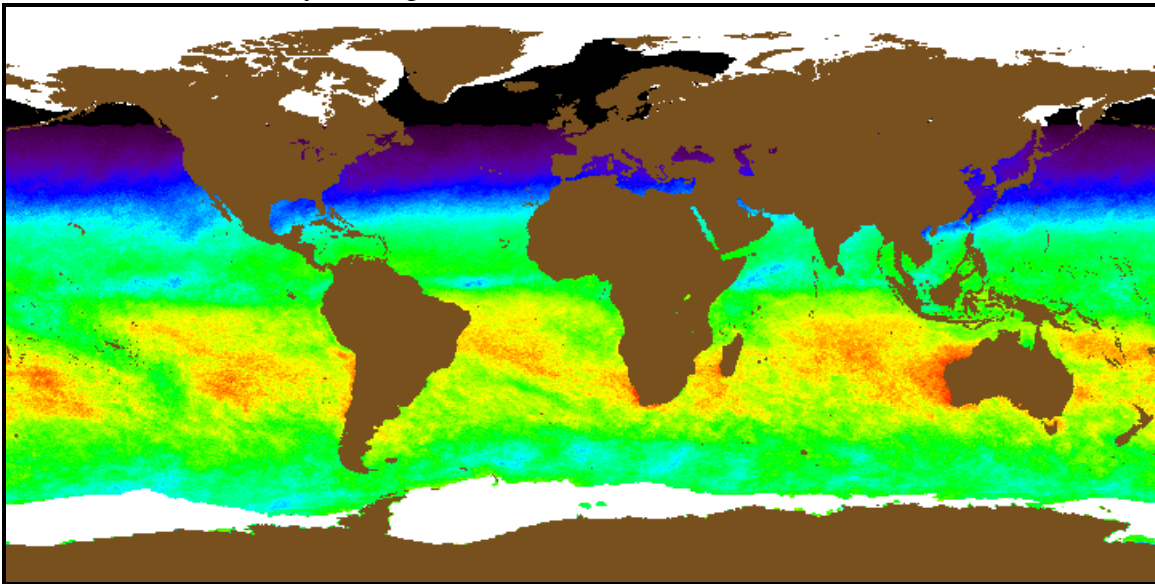


Figure 4: SeaWiFS (solid) and ISCCP (dotted) Global Distribution of PAR

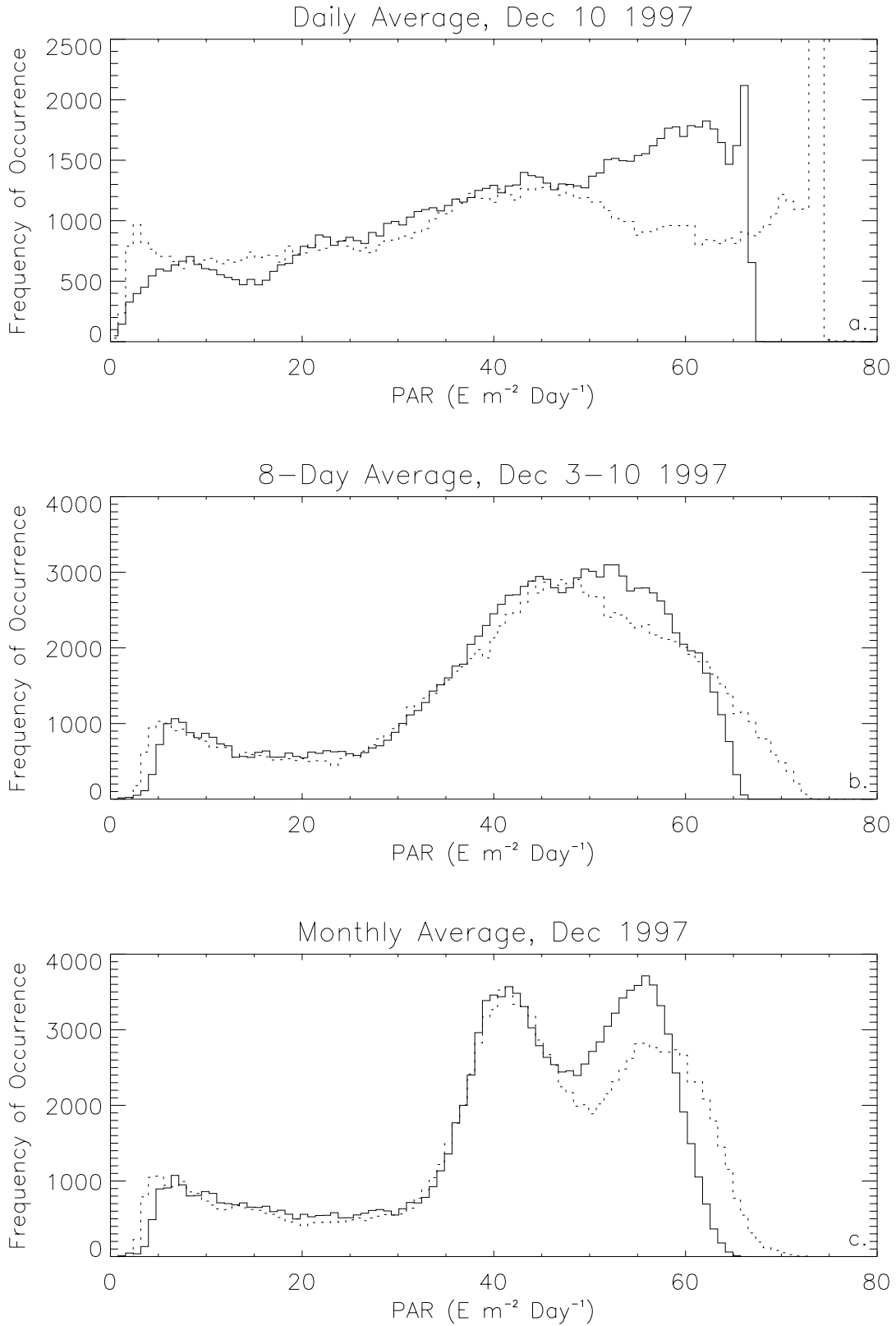


Figure 5: SeaWiFS PAR versus *in situ* PAR, Daily Average

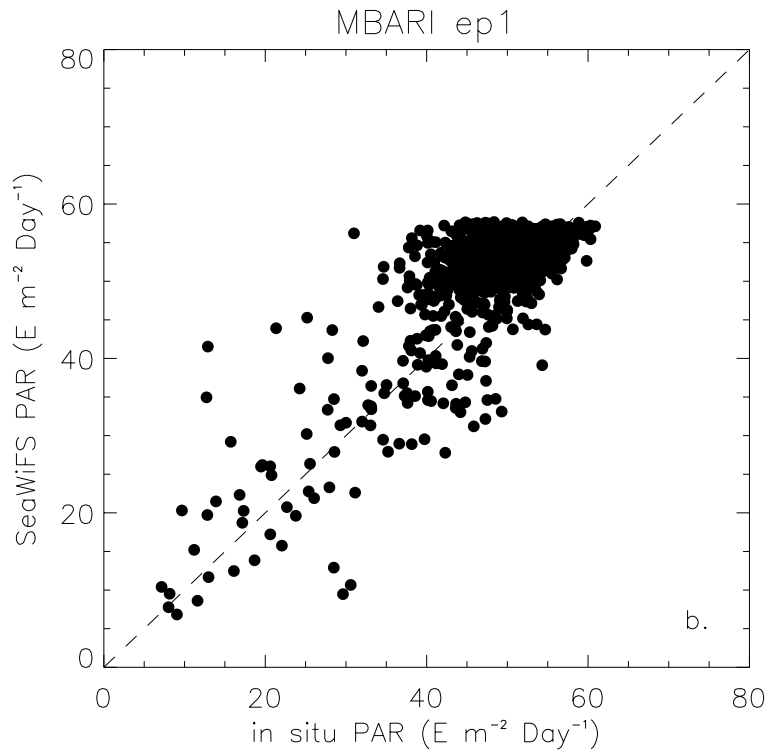
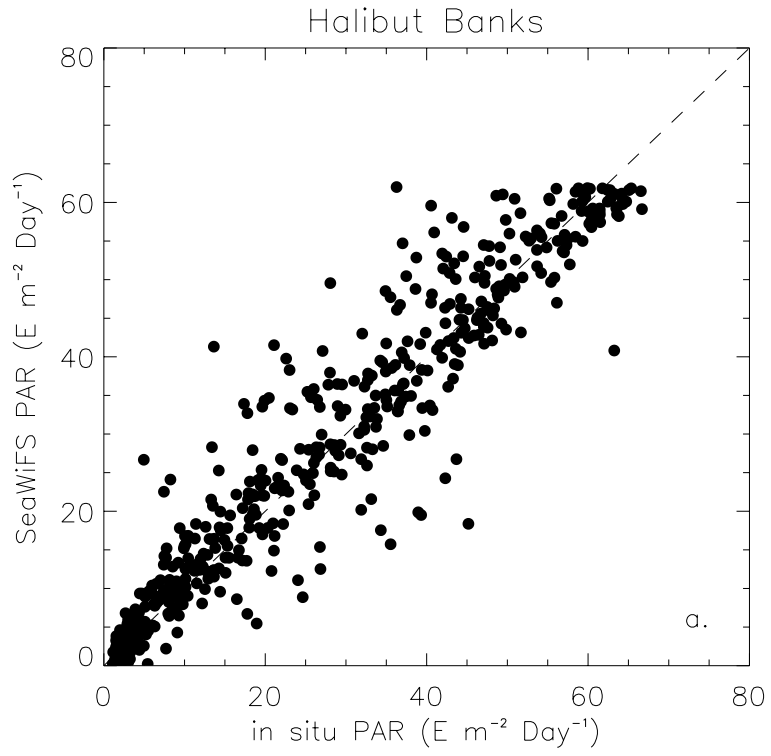


Figure 6: SeaWiFS PAR versus *in situ* PAR, 8-Day Average

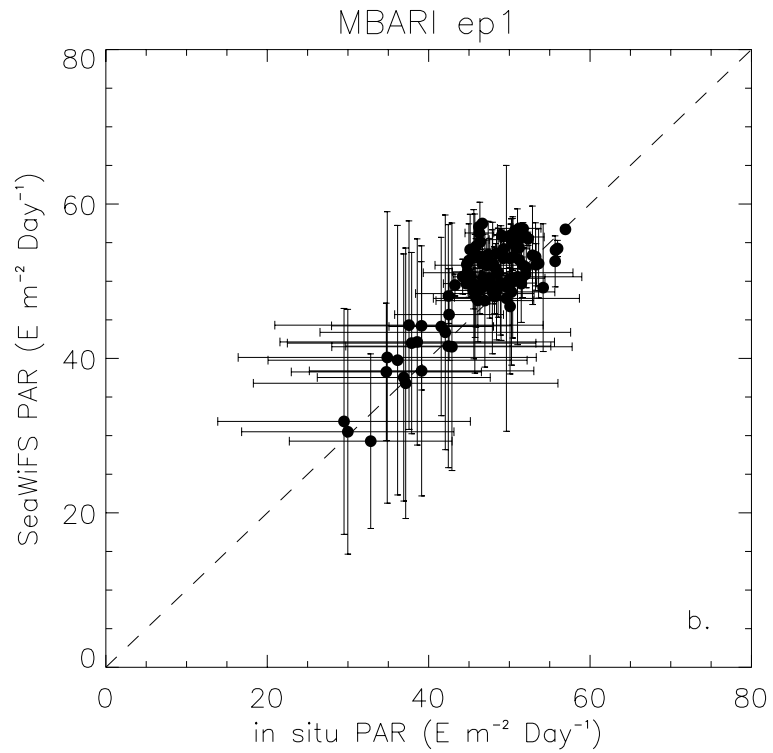
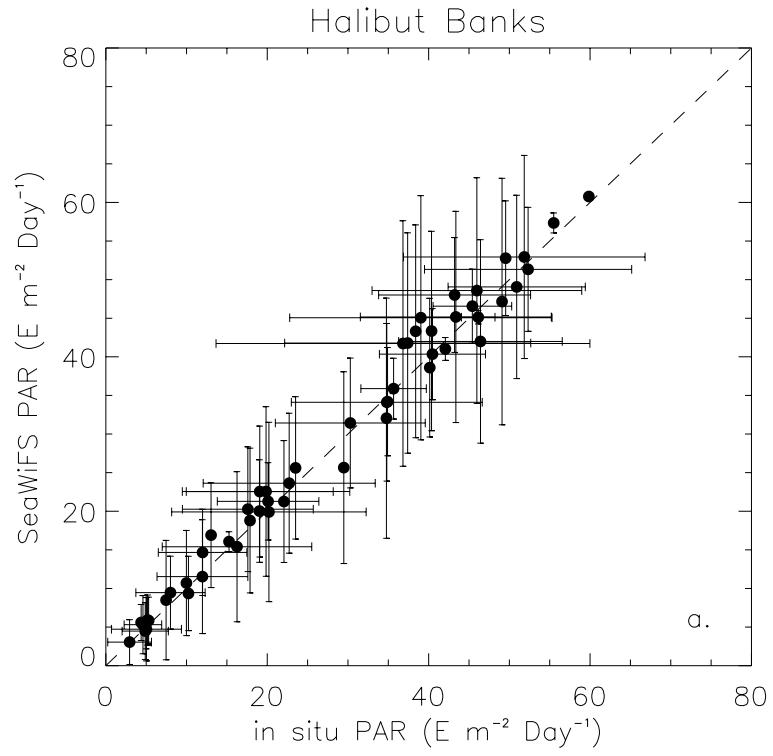


Figure 7: SeaWiFS PAR versus *in situ* PAR, Monthly Average

